Critical superparamagnetic/single-domain grain sizes in interacting magnetite particles: implications for magnetosome crystals

Adrian R. Muxworthy[1],* **and Wyn Williams[2]**

[1]*Department of Earth Science and Engineering, Imperial College London, South Kensington Campus, London SW7 2AZ, UK*
[2]*Grant Institute of Earth Science, University of Edinburgh, Kings Buildings, West Mains Road, Edinburgh EH9 3JW, UK*

Magnetotactic bacteria contain chains of magnetically interacting crystals (magnetosome crystals), which they use for navigation (magnetotaxis). To improve magnetotaxis efficiency, the magnetosome crystals (usually magnetite or greigite in composition) should be magnetically stable single-domain (SSD) particles. Smaller single-domain particles become magnetically unstable owing to thermal fluctuations and are termed superparamagnetic (SP). Previous calculations for the SSD/SP threshold size or blocking volume did not include the contribution of magnetic interactions. In this study, the blocking volume has been calculated as a function of grain elongation and separation for chains of identical magnetite grains. The inclusion of magnetic interactions was found to decrease the blocking volume, thereby increasing the range of SSD behaviour. Combining the results with previously published calculations for the SSD to multidomain threshold size in chains of magnetite reveals that interactions significantly increase the SSD range. We argue that chains of interacting magnetosome crystals found in magnetotactic bacteria have used this effect to improve magnetotaxis.

Keywords: magnetotactic bacteria; magnetosome crystals; superparamagnetic behaviour; blocking volume; magnetotaxis

1. INTRODUCTION

Magnetotactic bacteria contain chains of magnetic crystals (magnetosome crystals) made usually of magnetite (Fe_3O_4) and occasionally of greigite (Fe_3S_4). As the primary purpose of these magnetosome crystals is thought to be for navigation (magnetotaxis), natural selection should ensure that the magnetosome crystals provide a strong magnetic signal to maximize their efficiency (Kopp & Kirschvink 2008). The magnetic state that best exhibits this quality is the stable single-domain (SSD) state. The magnetic state of a crystal is strongly dependent on both size and shape. Although very small grains are single domain (SD) *sensu stricto*, they are no longer magnetically stable owing to thermal agitation and display superparamagnetic (SP) behaviour. Larger grains above the SD threshold size nucleate complex non-uniform or multidomain (MD) structures, which leads to inefficient magnetotaxis.

The critical sizes for the SSD range are also of interest to other scientists including material scientists and Earth scientists, because SSD grains display the highest recording fidelity, and because the easily identified magnetic characteristics of SSD grains are useful indicators of grain size.

In a much-cited paper, Butler & Banerjee (1975) calculated both the SP to SSD critical size and the SD to MD critical size, as functions of the grain-elongation axial ratio (AR; short axis/long axis or width/length) for individual parallelepiped magnetite crystals. As geologists, they were interested in magnetite owing to its natural abundance in rocks and its large spontaneous magnetization (M_S).

The analytically determined critical-size estimates of Butler & Banerjee (1975) have been refined through the application of Brown's (1963) numerical micromagnetic equations to the problem. Both the SP to SSD transition size (Winklhofer *et al.* 1997; Muxworthy *et al.* 2003) and the SD to MD transition size (e.g. Fabian *et al.* 1996; Newell & Merrill 1999; Witt *et al.* 2005; Muxworthy & Williams 2006) have been re-examined for individual grains.

It is common to assess the domain state of magnetosome crystals by plotting their length versus AR against the domain-state phase diagrams (Thomas-Keprta *et al.* 2000). By determining the SSD to MD critical-size calculations for magnetostatically interacting chains of elongated magnetite grains, Muxworthy & Williams (2006) demonstrated that it is flawed to compare such observations with boundaries derived for individual magnetosome crystals, because magnetosome crystals nearly always occur in magnetostatically interacting

chains. Muxworthy & Williams (2006) showed that magnetostatic interaction fields are sufficient to cause the largest observed magnetosome crystals found in living bacteria (length of 250 nm (AR = 0.84); Lins *et al.* 2005) to be in an SSD state; without magnetostatic interactions, they would be in an MD state having a far lower magnetotaxis efficiency. The fossil record produces one exception; Schumann *et al.* (2008) report a spearhead-like magnetosome-crystal magnetite fossil up to 4000 nm in length (AR ∼ 0.4).

Most of the magnetosome crystals reported in the literature are in the size range of 35–120 nm (Bazylinski & Frankel 2004), and are above the SP/SSD threshold size for individual grains of cubic magnetite, i.e. 25–30 nm (Dunlop & Özdemir 1997), yet there are still reports of magnetosome crystals that plot well within the SP region; for example Arató *et al.* (2005) reported magnetosome crystals less than 20 nm in length.

Are these small magnetosome crystals really behaving in a SP manner, or do magnetic interactions reduce the SP/SSD boundary? Studies examining other magnetic problems have shown that interactions lower the SP/SSD boundary (Muxworthy 2001). In this paper, we address this issue of the contribution of magnetic interactions to the SP/SSD threshold size for chains of magnetosome crystals.

We use a numerical model to quantify the effect of interactions. We model interacting elongated parallelepipeds as an approximation to magnetosome crystals. For individual grains, parallelepipeds have been shown to yield slightly lower estimates for the SSD/MD threshold size than numerical estimates for more magnetosome-like morphologies (Witt *et al.* 2005), yet the differences are small compared with the effect of magnetic interactions (Muxworthy & Williams 2006). Exact quantification of these differences is not possible as the absolute values for the SSD/MD threshold size for individual parallelepipeds determined by Witt *et al.* (2005) are less than those of Muxworthy & Williams (2006). In fact, the parallelepiped threshold predictions of Muxworthy & Williams (2006) are closer to the magnetosome-like morphology threshold-size predictions of Witt *et al.* (2005) than to the latter's predictions for parallelepipeds. This difference between the two model predictions for parallelepipeds is most likely because Witt *et al.* (2005) used a conjugate-gradient (CG) rather than dynamic numerical solver as used by Muxworthy & Williams (2006); fast CG solvers are now generally considered to produce less robust solutions than dynamic solvers (Suess *et al.* 2002).

2. THE MAGNETIC INTERACTION FIELDS IN THERMALLY ACTIVATED SD SYSTEMS

In systems of interacting SD grains, both SP and SSD grains contribute to the interaction field. The magnetic interaction field generated by an SSD grain is constant during the rotation of a neighbouring interacting SP or SSD grain. This makes it possible to treat magnetic interaction fields due to SSD grains as effectively static (Spinu & Stancu 1998). The effect of magnetostatic interactions due to SSD grains is to increase/decrease

the H_K, the (micro)coercive force of a crystal, by the interaction field, $\pm H_S$ (Dunlop & West 1969).

For SP grains, the situation is more complicated. The behaviour of a magnetic assembly of SP particles falls into one of three regimes depending on the interparticle interactions (Dormann *et al.* 1997): (i) pure SP (non-interacting case), (ii) a SP state modified by interactions, and (iii) a collective state. The properties of state (iii), called the glass collective state (Dormann *et al.* 1999), are close to those of spin glasses showing a phase transition. This state is presently not fully understood and there is no analytical model for the collective state. However, for the purposes of this model, it is necessary to consider only state (ii), an SP state modified by magnetostatic interactions.

For the interaction regime, near the blocking volume or temperature where relaxation is important in the system, the interaction field due to SP grains fluctuates at a high rate. These dynamic interactions are qualitatively different from static ones. Dynamic systems are not in thermodynamic equilibrium and hence cannot be directly modelled using Boltzmann statistics. Several approaches have been developed to address this problem (Dormann *et al.* 1988). These models show that the effect of interactions due to SP grains is to increase the relaxation time t_m, given by Néel (1949)

$$t_m = \tau_n \exp(-Eg/kT) \qquad (2.1)$$

by increasing the energy barrier $E_B = E_A$ (where E_A is the anisotropy energy barrier), by an amount E_{int}, i.e. $E_B = E_A + E_{int}$, where k is Boltzmann's constant; T is the temperature; and τ_0 is the atomic reorganization time (approx. 10^{-9}) (Worm 1998). The relaxation time t_m can be a few nanoseconds for laboratory experiments to gigayears for geological samples.

For an SD assemblage with both dynamic SP and static SSD interactions, the standard blocking volume, v_b, is modified from the non-interacting case, given by Dunlop & Özdemir (1997)

$$v_b = \frac{2kT \ln(t_w/\tau_0)}{\mu_0 M_s H_K}, \qquad (2.2)$$

to the interacting one (Muxworthy 2001),

$$v_b = \frac{-E_{int} + 2kT \ln(t_m + \tau_0)}{\mu_0 M_s (H_K \pm H_s)}, \qquad (2.3)$$

where μ_0 is the permeability of free space.

3. BLOCKING VOLUME FOR A CHAIN OF IDENTICAL GRAINS: A MODEL FOR MAGNETOSOME CRYSTALS

For an SD assemblage with a distribution of grain volumes, it is necessary to calculate both E_{int} and H_S (Muxworthy 2001). However, equation (2.1) can be simplified for chains of interacting identical SD grains. If the assumption is made that every grain is either blocked or unblocked, i.e. all the particles including the end grains exhibit identical behaviour, then the blocking volume is simply the case where the

magnetostatic interaction fields alone, i.e. $E_{int} \equiv 0$, are sufficient to overcome the thermal fluctuation fields.

The chains of grains just below the blocking volume will not display true SP behaviour but will still be in a dynamic, magnetically unstable state. Consider the following scenario: if the grains unblock, then E_{int} will increase causing blocking, yet upon blocking the magnetostatic interaction field will not be strong enough to keep the chain blocked, and the chain will unblock, and so on. Hence, a chain of identical grains will constantly block and unblock, making the chain magnetically unstable and effectively SP in behaviour. Therefore, all that is required to find the blocking volume of a chain of identical grains is the value of H_S, such that $H_K \pm H_S$ overcomes thermal fluctuations.

There are two methods of determining $H_K \pm H_S$: (i) calculate H_K analytically and determine H_S numerically for a chain of interacting parallelepipeds or (ii) determine the coercive force H_C ($=H_K \pm H_S$) numerically for a chain of interacting parallelepipeds. The first approach will yield slightly higher H_C estimates, as it essentially estimates the switching field of one particle in a 'magnetically static' interacting chain, whereas the second method allows for more complex mechanisms of chain reversal such as fanning (Kneller 1969). We consider the second approach in this paper.

3.1. The micromagnetic algorithm

To determine H_C through magnetic hysteresis simulation, we have implemented an identical combination micromagnetic algorithm, which we have previously used (Muxworthy & Williams 2004, 2006; Williams *et al.* 2006). The program is a finite-difference model that divides the magnetic structure into a number of sub-cubes. Each sub-cube represents the averaged magnetization direction of many hundreds of atomic magnetic dipole moments. The orientation of each sub-cube can vary.

The approach combines both a minimum energy CG algorithm (Williams & Dunlop 1989) and a dynamic algorithm, which follows the torque of a magnetic moment according to the Landau–Lifshitz–Gilbert (LLG) equation (Suess *et al.* 2002). The reasoning behind this approach is that the dynamic algorithm gives the more rigorous solution since the magnetization between stable states must follow a physically reasonable path dictated by the LLG equation of motion, yet it is relatively slow compared with the CG method. In this combination algorithm, we use the CG algorithm to rapidly generate an initial guess for the magnetic structure, by minimizing the total magnetic energy, which is the sum of the exchange energy, the magnetostatic energy and the magnetocrystalline anisotropy energy (Brown 1963). The solution is then put into the dynamic solver. This increases the efficiency of the algorithm by roughly an order of magnitude compared with the dynamic solver alone. This combined method produces a more robust solution, because it minimizes the torque on each magnetic moment. The CG method by itself only minimizes the total energy. The dynamic solver produces lower energy states than the CG algorithm alone. We use fast Fourier transforms (FFTs) to calculate
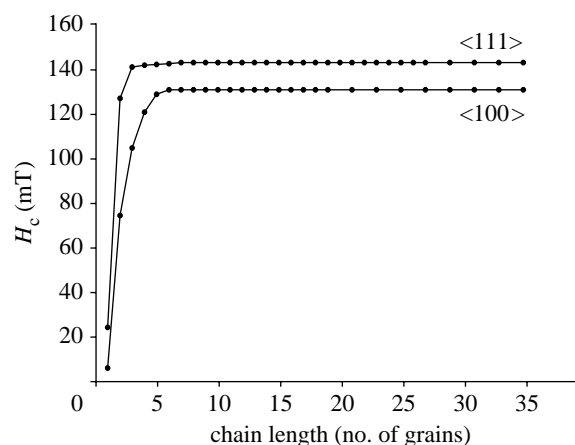
Figure 1. Coercive force versus chain length for simulated chains of touching cubic grains of magnetite. The coercive force was determined from simulated hysteresis loops with a field angle of 0° with respect to the chain orientation.
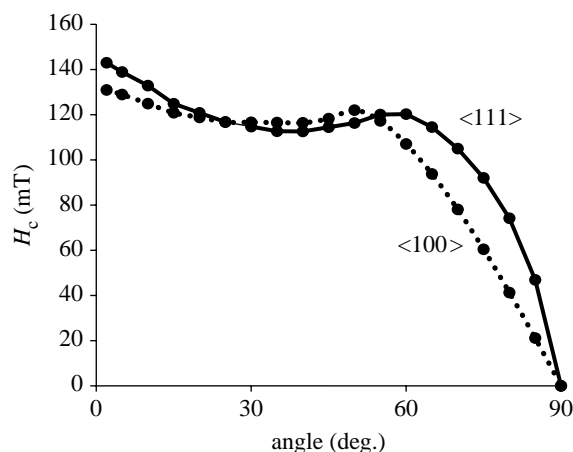

Figure 2. Coercive force versus magnetic field orientation for simulated chains of touching cubic grains of magnetite. Two configurations are shown: (i) the magnetocrystalline easy-axis anisotropy aligned along the chain length ($\langle 1\,1\,1 \rangle$) and (ii) the hard axis aligned with the chain length ($\langle 1\,0\,0 \rangle$). The chain length in the simulations was 7.

the magnetostatic energy, which allows the high resolution needed to examine arrays of interacting grains.

In our calculation of H_C, we considered chains with various spacings from non-interacting grains ($s = \infty$) to touching grains with a spacing/length ratio $s = 0.0$, where the length is the long axis of the parallelepipeds. The model includes both magnetite's cubic magnetocrystalline anisotropy and a 'shape anisotropy', which is calculated in the magnetostatic energy term.

3.2. Determining the coercive force for a chain of magnetite magnetosome crystals

In addition to magnetic interactions, chain length, grain elongation and intrinsic magnetocrystalline anisotropy, the coercive force H_C for a chain of magnetosome crystals depends on the field angle with respect to the chain-length extension, grain elongation and magnetocrystalline anisotropy orientation. The problem is simplified for magnetosome crystals as grain elongation and chain-length extension are
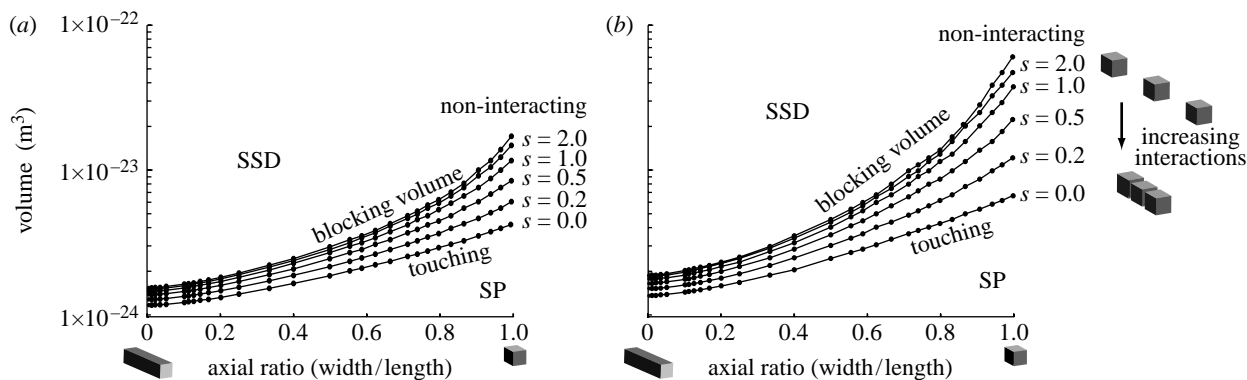
Figure 3. Blocking volume versus AR for chains of magnetite separated by different spacings (s=spacing/length). Two configurations are shown: (a) the magnetocrystalline easy-axis anisotropy aligned along the chain length ($\langle 1\,1\,1 \rangle$) and (b) the hard axis aligned with the chain length ($\langle 1\,0\,0 \rangle$). Relaxation time for (a) and (b) is t_m=60 s.
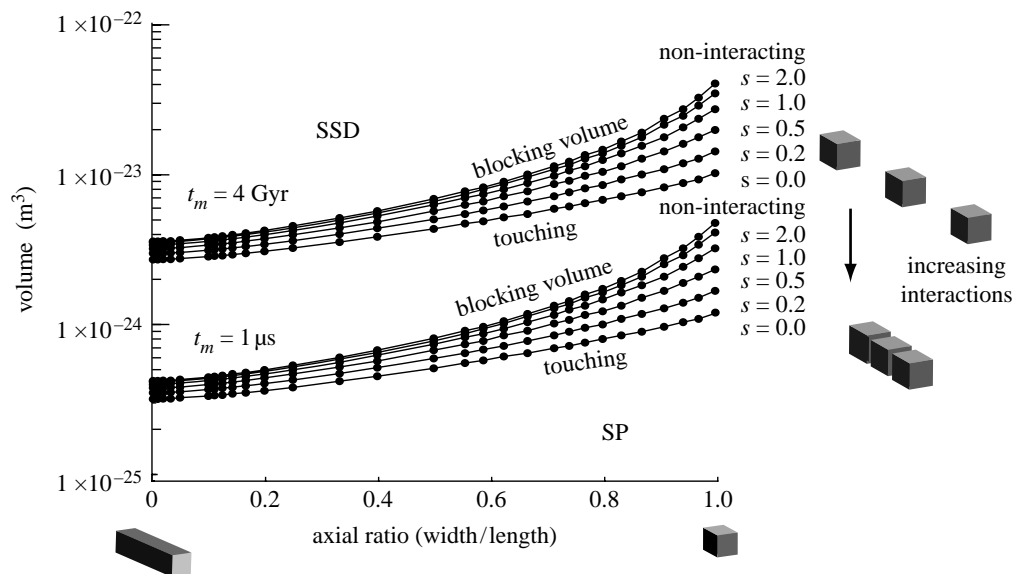

Figure 4. Blocking volume versus AR for chains of magnetite with different grains (s=spacing/length) and different relaxation times (t_m=4 Gyr and t_m=1 μs).

aligned. In addition, we consider only the two extreme cases of crystal orientation, i.e. the crystallographic $\langle 1\,1\,1 \rangle$ and $\langle 1\,0\,0 \rangle$ axes aligned with the chain. The two orientations are the easy and hard magnetocrystalline anisotropy axes, respectively. Magnetite magnetosome-crystal chains are commonly observed to align along the $\langle 1\,1\,1 \rangle$ axis (Kopp 2007).

To determine the coercive force H_C, first, we need to determine the minimum chain length required to remove chain-length dependency of H_C. In figure 1, we plot H_C versus chain length for chains of touching, symmetrical grains (AR=1) with both the magneto-crystalline anisotropy $\langle 1\,1\,1 \rangle$ and $\langle 1\,0\,0 \rangle$ orientations aligned along the chain length. For both configurations, above a chain length of 7, H_C becomes independent of the chain length. For the rest of the calculations in this paper, a chain length of 7 was used. Aligning the cubic magnetocrystalline easy-axis anisotropy with the chain length enhances H_C.

Second, we must also consider the field angle with respect to the chain length. In figure 2, H_C is seen to be highly dependent on the magnetic field angle with respect to the chain orientation, for chains of touching cubic grains (AR=1) for both the magnetocrystalline anisotropy $\langle 1\,1\,1 \rangle$ and $\langle 1\,0\,0 \rangle$ configurations. However, to determine the blocking volume, it is not necessary to integrate over a distribution of orientations, as we are only interested in determining the size of the energy barrier (or H_C) to be overcome by scalar thermal fluctuations. Therefore, we need only consider switching between the zero-field easy-axis positions, that is, for interacting chains with the magnetization aligned along the chain; we need only consider a field angle of 0° (figure 2).

The blocking volume was determined using equation (2.3) for magnetite with t_m=60 s and plotted against grain volume (figure 3) by, first, numerically calculating H_C for a range of ARs and grain spacings. For the non-interacting case, i.e. $s=\to\infty$, v_b decreases with increasing elongation (decreasing AR). This is in agreement with previous calculations (Butler & Banerjee 1975; Winklhofer *et al.* 1997). Aligning the magnetocrystalline easy axis with the chain length ($\langle 1\,1\,1 \rangle$ configuration; figure 3a) increases H_C and, hence, decreases v_b with respect to the hard-axis alignment configuration ($\langle 1\,0\,0 \rangle$; figure 3b).
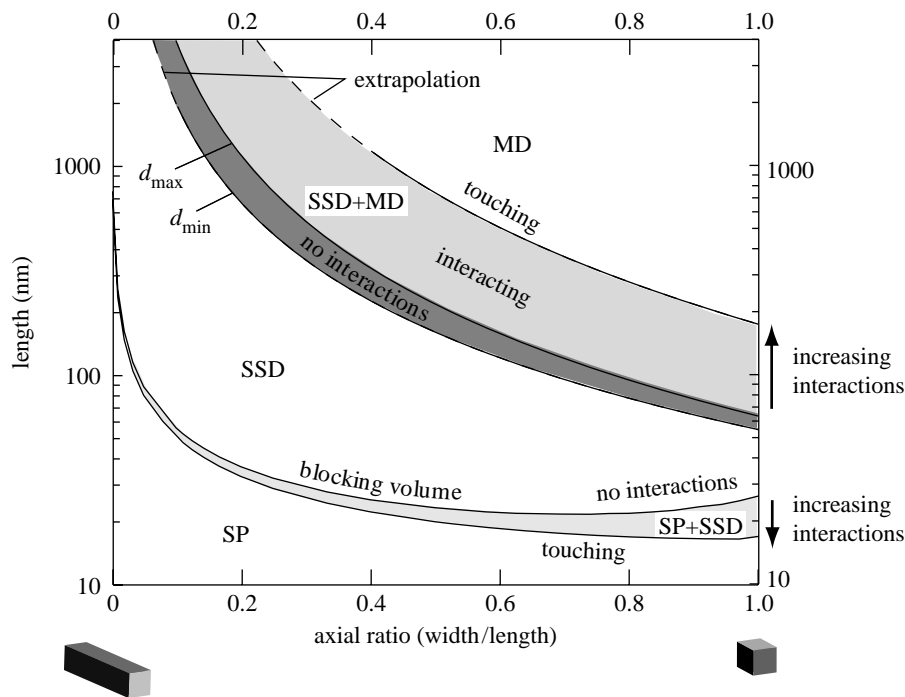
Figure 5. SSD ranges for individual grains and chains of interacting magnetosome crystals. Combining the work from this study for the SP to SSD limit ($t_m = 60$ s and the chain aligned in the $\langle 1\,1\,1 \rangle$ configuration) with the models of Muxworthy & Williams (2006) for the SD to MD transition size. Using the format of Butler & Banerjee (1975), length (long axis) rather than volume is plotted versus AR for various grain spacings/length ratios. The use of the length makes for easier comparison with Butler & Banerjee (1975), but the figure is a little more complicated to understand, because, on moving horizontally across the figure, the volume of the grains changes, i.e. there is a change in both shape and volume contributing to the critical boundaries. Hence, the blocking size appears to go up with elongation, unlike in figures 3 and 4. For non-interacting grains, there is a range of grain sizes marked by $d_{\min}$ and $d_{\max}$, where both SD and MD domain states are possible.

In all the interacting models, H_S (equation (2.3)) was positive. Generally, for systems with two- and three-dimensional magnetostatic interaction fields, H_S is negative (Muxworthy & Williams 2004), but here it is positive because the particles are in a chain producing a linear interaction field. Positive magnetostatic interactions effectively increase H_C, resulting in a reduction of v_b (figure 3), i.e. interactions decrease the SP to SSD transition boundary. As the degree of interaction increases, v_b decreases, this effect being most pronounced for high AR.

For comparison, v_b was determined for both $t_m = 1$ μs and 4 Gyr (figure 4). As was shown by Butler & Banerjee (1975) for individual grains, increasing the relaxation time results in an increase in the blocking volume. The longer time scale was chosen for geologists who are interested in magnetic stabilities over the age of the Earth and the Solar System, and the shorter as an extreme case to demonstrate variability in t_m.

4. CONCLUSIONS

Combining the results of this study with that of Muxworthy & Williams (2006), it is possible to display critical-size ranges for chains of interacting elongated SD grains, in addition to individual elongated SD grains (figure 5).

The interactions both decrease the SP to SSD transition size for chains of SD grains and increase the SSD to MD transition size, significantly expanding the SSD range. For example, for AR=1 and $t_m = 60$ s, the non-interacting SSD range is 17 nm < length < 73 nm, which increases to 12 nm < length < 198 nm for chains of touching grains.

The range of magnetite-bearing magnetosome-crystal sizes for living bacteria varies from a maximum length of 250 nm (AR=0.84) to lengths of less than 20 nm (Taylor & Barry 2004; Arató *et al.* 2005; Lins *et al.* 2005), though the majority lie between 35 and 120 nm (Bazylinski & Frankel 2004) in length. Comparing the domain-state phase diagram (figure 5) with the published observational data, we suggest that magnetotactic bacteria have used magnetic interactions for magnetosome-crystal size optimization.

There is one exception, which is found in the fossil record (Schumann *et al.* 2008). Schumann *et al.* (2008) observed spearhead-like magnetosome-crystal fossil up to 4000 nm in length (AR ∼ 0.4) in sediments *ca* 55.6 Myr old. According to figure 5, these magnetosome crystals should reside in a MD state. Generally, however, owing to the increased magnetic stability of magnetosome-crystal chains, the magnetic signal carried by fossil magnetotactic bacteria will be highly stable and geologically reliable.

REFERENCES

Arató, B., Szányi, Z., Flies, C., Schuler, D., Frankel, R. B., Buseck, P. R. & Pósfai, M. 2005 Crystal-size and

shape distributions of magnetite from uncultured magnetotactic bacteria as a potential biomarker. *Am. Min.* **90**, 1233–1240. (doi:10.2138/am.2005.1778)

Bazylinski, D. A. & Frankel, R. B. 2004 Magnetosome formation in prokaryotes. *Nat. Rev. Microbiol.* **2**, 217–230. (doi:10.1038/nrmicro842)

Brown Jr, W. F. 1963 *Micromagnetics.* New York, NY: Wiley.

Butler, R. F. & Banerjee, S. K. 1975 Theoretical single-domain grain size range in magnetite and titanomagnetite. *J. Geophys. Res.* **80**, 4049–4058. (doi:10.1029/JB080i029p04049)

Dormann, J. L., Bessais, L. & Fiorani, D. 1988 A dynamic study of small interacting particles—superparamagnetic model and spin-glass laws. *J. Phys. C* **21**, 2015–2034. (doi:10.1088/0022-3719/21/10/019)

Dormann, J. L., Fiorani, D. & Tronc, E. 1997 Magnetic relaxation in fine-particle systems. *Adv. Chem. Phys.* **98**, 283–494. (doi:10.1002/9780470141571.ch4)

Dormann, J. L., Fiorani, D. & Tronc, E. 1999 On the models for interparticle interactions in nanoparticle assemblies: comparison with experimental results. *J. Magnet. Magn. Mater.* **202**, 251–267. (doi:10.1016/S0304-8853(98)00627-1)

Dunlop, D. J. & Özdemir, Ö. 1997 *Rock magnetism: fundamentals and frontiers.* Cambridge studies in magnetism. Cambridge, UK: Cambridge University Press.

Dunlop, D. J. & West, G. F. 1969 An experimental evaluation of single-domain theories. *Rev. Geophys.* **7**, 709–757. (doi:10.1029/RG007i004p00709)

Fabian, K., Kirchner, A., Williams, W., Heider, F., Leibl, T. & Huber, A. 1996 Three-dimensional micromagnetic calculations for magnetite using FFT. *Geophys. J. Int.* **124**, 89–104. (doi:10.1111/j.1365-246X.1996.tb06354.x)

Kneller, E. 1969 Fine particle theory. In *Magnetism and metallurgy* (eds A. Berkowitz & E. Kneller), pp. 366–472. New York, NY: Academic Press.

Kopp, R. E. 2007 *The identification and interpretation of microbial biogeomagnetism*, p. 191. Pasadena, CA: California Institute of Technology.

Kopp, R. E. & Kirschvink, J. L. 2008 The identification and biogeochemical interpretation of fossil magnetotactic bacteria. *Earth Sci. Rev.* **86**, 42–61. (doi:10.1016/j.earscirev.2007.08.001)

Lins, U., McCartney, M. R., Farina, M., Frankel, R. B. & Buseck, P. R. 2005 Habits of magnetosome crystals in coccoid magnetotactic bacteria. *Appl. Environ. Microbiol.* **71**, 4902–4905. (doi:10.1128/AEM.71.8.4902-4905.2005)

Muxworthy, A. R. 2001 Effect of grain interactions on the frequency dependence of magnetic susceptibility. *Geophys. J. Int.* **144**, 441–447. (doi:10.1046/j.1365-246x.2001.00342.x)

Muxworthy, A. R. & Williams, W. 2004 Distribution anisotropy: the influence of magnetic interactions on the anisotropy of magnetic remanence. In *Magnetic fabric: methods and applications* (eds F. Martín-Hernández, C. M. Lüneburg, C. Aubourg & M. Jackson), pp. 37–47. London, UK: Geological Society.

Muxworthy, A. R., Dunlop, D. J. & Williams, W. 2003 High-temperature magnetic stability of small magnetite particles. *J. Geophys. Res.* **108**, 2281. (doi:10.1029/2002JB002195)

Muxworthy, A. R. & Williams, W. 2006 Critical single-domain/multidomain grain-sizes in non-interacting and interacting elongated magnetite particles: implications for magnetosomes. *J. Geophys. Res.* **111**, B12S12. (doi:10.1029/2006JB004588)

Néel, L. 1949 Théorie du trainage magnétique des ferromagnétiques en grains fins avec applications aux terres cuites. *Ann. Géophys.* **5**, 99–136.

Newell, A. J. & Merrill, R. T. 1999 Single-domain critical sizes for coercivity and remanence. *J. Geophys. Res.* **104**, 617–628. (doi:10.1029/1998JB900039)

Schumann, D. *et al.* 2008 Gigantism in unique biogenic magnetite at the Paleocene–Eocene thermal maximum. *Proc. Natl Acad. Sci. USA* **105**, 17 648–17 653. (doi:10.1073/pnas.0803634105)

Spinu, L. & Stancu, A. 1998 Modelling magnetic relaxation phenomena in fine particles systems with a Preisach–Neel model. *J. Magnet. Magn. Mater.* **189**, 106–114. (doi:10.1016/S0304-8853(98)00205-4)

Suess, D., Tsiantos, V., Schrefl, T., Fidler, J., Scholz, W., Forster, H., Dittrich, R. & Miles, J. J. 2002 Time resolved micromagnetics using a preconditioned time integration method. *J. Magnet. Magn. Mater.* **248**, 298–311. (doi:10.1016/S0304-8853(02)00341-4)

Taylor, A. P. & Barry, J. C. 2004 Magnetosomal matrix: ultrafine structure may template biomineralization of magnetosomes. *J. Microsc.* **213**, 180–197. (doi:10.1111/j.1365-2818.2004.01287.x)

Thomas-Keprta, K. L., Bazylinski, D. A., Kirschvink, J. L., Clemett, S. J., McKay, D. S., Wentworth, S. J., Vali, H., Gibson Jr, E. K. & Romanek, C. S. 2000 Elongated prismatic magnetite crystals in ALH 84001 carbonate globules: potential Martian magnetofossils. *Geochim. Cosmochim. Acta* **64**, 4049–4081. (doi:10.1016/S0016-7037(00)00481-6)

Williams, W. & Dunlop, D. J. 1989 Three-dimensional micromagnetic modelling of ferromagnetic domain structure. *Nature* **337**, 634–637. (doi:10.1038/337634a0)

Williams, W., Muxworthy, A. R. & Paterson, G. A. 2006 Configurational anisotropy in single-domain and pseudo-single-domain grains of magnetite. *J. Geophys. Res.* **111**, B12S13. (doi:10.1029/2006JB004556)

Winklhofer, M., Fabian, K. & Heider, F. 1997 Magnetic blocking temperatures of magnetite calculated with a three-dimensional micromagnetic model. *J. Geophys. Res.* **102**, 22 695–22 709. (doi:10.1029/97JB01730)

Witt, A., Fabian, K. & Bleil, U. 2005 Three-dimensional micromagnetic calculations for naturally shaped magnetite: octahedra and magnetosomes. *Earth Planet. Sci. Lett.* **233**, 311–324. (doi:10.1016/j.epsl.2005.01.043)

Worm, H.-U. 1998 On the superparamagnetic-stable single domain transition for magnetite, and frequency dependence of susceptibility. *Geophys. J. Int.* **133**, 201–206. (doi:10.1046/j.1365-246X.1998.1331468.x)